



PUBLISHED BY INSTITUTE OF PHYSICS PUBLISHING FOR SISSA/ISAS

RECEIVED: November 8, 2019

ACCEPTED: November 8, 2019

JHEP00(2009)000

Spectrum of Spin 1 Dirac Operators on the Fuzzy 2-Sphere

Sanatan Digal*The Institute of Mathematical Sciences, CIT Campus, Taramani, Chennai 600 113,**India**E-mail: digal@imsc.res.in***Pramod Padmanabhan***Department of Physics, Syracuse University, Syracuse, NY 13244-1130, USA**The Institute of Mathematical Sciences, CIT Campus, Taramani, Chennai 600 113,
India**E-mail: ppadmana@syr.edu*

ABSTRACT: We numerically find out the spectrum of the 3 spin 1 Dirac operators found in [1]. We give an analytic and numerical proof that they are unitarily inequivalent. Since these operators come paired with an anticommuting chirality operator, we find their spectrums to resemble those of fermions with positive and negative eigenvalues along with a number of zero modes. We give a method to count the number of zero modes which can be extended to higher spins on S_F^2 . An universal relation between the energy eigenvalues of the spin 1 Dirac operator and their multiplicities is found. This helps us predict the energy eigenvalues for an arbitrarily large cut-off L , a problem which is computationally difficult to handle.

KEYWORDS: Non-Commutative Geometry, Matrix Models, Field Theories in Lower Dimensions.

Contents

1. Introduction	1
2. Geometry of S_F^2	2
3. Construction of the Dirac Operators	3
4. Analytic results of the spectrums of the spin $\frac{1}{2}$ and spin 1 Dirac operators	6
4.1 Number of positive eigenvalues and Zero modes for the spin 1 Dirac operator	7
4.2 Remarks on the other two Dirac operators for the spin 1 case	8
5. Numerical Results	9
6. Conclusions	11
7. Acknowledgements	13

1. Introduction

Fuzzy spaces provide an attractive, alternative way to discretize spacetime and thus help regularize field theories on such spaces. Its interesting feature is the fact that this method preserves the symmetries of the continuum spacetimes even at the discrete level which are broken in lattice regularization techniques.

Such fuzzy spaces are studied using the noncommuting algebra of functions defined on them. One such widely studied model is the fuzzy sphere S_F^2 [2, 3]. Several works on numerical simulations of scalar fields and gauge fields on S_F^2 have been done. [4, 5, 6, 7, 8, 9].

There have also been interesting attempts to extend physics to other such fuzzy spaces with higher genuses [10] and more exotic looking surfaces [11, 12]. But here we will consider only S_F^2 .

In Connes' approach to noncommutative geometry [13], the Dirac operator gains fundamental significance as part of the spectral triple in formulating the spectral action principle. Such a spectral action has been considered recently [14] for the Dirac operator of a spin $\frac{1}{2}$ particle. The operator used by them corresponds to the one constructed in [16]. In this work we will consider Dirac operators constructed with the help of Ginsparg-Wilson(GW) algebras. This approach provides an elegant way to extend the construction of Dirac operators to all spins as studied in [1], where it was also found that several such Dirac operators exist for the case of each spin j .

We consider the spin 1 case and numerically compute the spectrum of the 3 Dirac operators. We also analytically compute the traces of these 3 operators and find that two of them have non-zero trace showing the existence of unpaired eigenstates(zero modes). One of them is traceless. Rather surprisingly, the spectrums are found to be different, both numerically and, analytically from the trace formulas, thereby establishing the unitary inequivalence of the three operators. The spectrum of the traceless Dirac operator is studied in detail. The eigenvalues are plotted as a function of their degeneracy. This is done for values of the cut-off, L for which we could compute the eigenvalues numerically. We then fit this data with curves for each L and find that a quadratic function fits it. This fit extends rather amazingly to all other values of L once we change the parameters in the fit which are functions of L . Thus this gives an universal relation between the energy and their degeneracy and helps predict the eigenvalues for any large value of L .

The paper is organized as follows. Section 2 briefly describes the noncommutative algebra on S_F^2 . We then recall the construction of Dirac operators using GW algebras in section 3. Here we also write down the 3 spin 1 Dirac operators which we will work with. The trace of these operators are found analytically. Their inequivalence provides a simple proof for the unitary inequivalence of the three operators. In section 4 we recall the spectrum of the spin $\frac{1}{2}$ Dirac operator and we study the properties of the spectrum of the spin 1 Dirac operator. In particular we provide an elegant way to count the number of zero modes of the traceless spin 1 Dirac operator for each cut-off L . The numerical results are presented in section 5. We conclude in section 6 with a few remarks and further speculations.

2. Geometry of S_F^2

The algebra for the fuzzy sphere is characterized by a cut-off angular momentum L and is the full matrix algebra $Mat(2L + 1) \equiv M_{2L+1}$ of $(2L + 1) \times (2L + 1)$ matrices. They can be generated by the $(2L + 1)$ -dimensional irreducible representation (IRR) of $SU(2)$ with the standard angular momentum basis. The latter is represented by the angular momenta L_i^L acting on the left on $Mat(2L + 1)$: If $\alpha \in Mat(2L + 1)$,

$$L_i^L \alpha = L_i \alpha \quad (2.1)$$

$$[L_i^L, L_j^L] = i\epsilon_{ijk}L_k^L \quad (2.2)$$

$$(L_i^L)^2 = L(L + 1)\mathbf{1} \quad (2.3)$$

where L_i are the standard angular momentum matrices for angular momentum L .

We can also define right angular momenta L_i^R :

$$L_i^R \alpha = \alpha L_i, \alpha \in M_{2L+1} \quad (2.4)$$

$$[L_i^R, L_j^R] = -i\epsilon_{ijk}L_k^R \quad (2.5)$$

$$(L_i^R)^2 = L(L + 1)\mathbf{1} \quad (2.6)$$

We also have

$$[L_i^L, L_j^R] = 0. \quad (2.7)$$

The operator $\mathcal{L}_i = L_i^L - L_i^R$ is the fuzzy version of orbital angular momentum. They satisfy the $SU(2)$ angular momentum algebra

$$[\mathcal{L}_i, \mathcal{L}_j] = i\epsilon_{ijk}\mathcal{L}_k \quad (2.8)$$

In the continuum, S^2 can be described by the unit vector $\hat{x} \in S^2$, where $\hat{x} \cdot \hat{x} = 1$. Its analogue on S_F^2 is $\frac{L_i^L}{L}$ or $\frac{L_i^R}{L}$ such that

$$\lim_{L \rightarrow \infty} \frac{L_i^{L,R}}{L} = \hat{x}_i. \quad (2.9)$$

This shows that $L_i^{L,R}$ do not have continuum limits. But $\mathcal{L}_i = L_i^L - L_i^R$ does and becomes the orbital angular momentum as $L \rightarrow \infty$:

$$\lim_{L \rightarrow \infty} L_i^L - L_i^R = -i(\vec{r} \wedge \vec{\nabla})_i. \quad (2.10)$$

3. Construction of the Dirac Operators

In algebraic terms, the GW algebra \mathcal{A} is the unital $*$ algebra over \mathbf{C} , generated by two $*$ -invariant involutions Γ, Γ' .

$$\mathcal{A} = \{\Gamma, \Gamma' : \Gamma^2 = \Gamma'^2 = 1, \Gamma^* = \Gamma, \Gamma'^* = \Gamma'\} \quad (3.1)$$

In any $*$ -representation on a Hilbert space, $*$ becomes the adjoint \dagger .

Consider the following two elements constructed out of Γ, Γ' :

$$\Gamma_1 = \frac{1}{2}(\Gamma + \Gamma'), \quad (3.2)$$

$$\Gamma_2 = \frac{1}{2}(\Gamma - \Gamma'). \quad (3.3)$$

It follows from Eq.(3.1) that $\{\Gamma_1, \Gamma_2\} = 0$. This suggests that for suitable choices of Γ, Γ' , one of these operators may serve as the Dirac operator and the other as the chirality operator provided they have the right continuum limits after suitable scaling.

For the spin 1 case the combination which leads to the desired Dirac and chirality operators were found in [1] and they are

$$D_1 = L \left(\frac{\Gamma_{L+1}^L - \Gamma_{L-1}^R}{2} \right), \quad (3.4)$$

$$D_2 = L \left(\frac{\Gamma_{L-1}^L - \Gamma_{L+1}^R}{2} \right) \quad (3.5)$$

and

$$D_3 = L \left(\frac{\Gamma_L^L - \Gamma_L^R}{2} \right). \quad (3.6)$$

with

$$\gamma_1 = \left(\frac{\Gamma_{L+1}^L + \Gamma_{L-1}^R}{2} \right), \quad (3.7)$$

$$\gamma_2 = \left(\frac{\Gamma_{L-1}^L + \Gamma_{L+1}^R}{2} \right) \quad (3.8)$$

and

$$\gamma_3 = \left(\frac{\Gamma_L^L + \Gamma_L^R}{2} \right) \quad (3.9)$$

as their corresponding chirality operators. In the above equations

$$\Gamma_{L+1}^L = \frac{2(\vec{\Sigma} \cdot \vec{L}^L + L + 1)(\vec{\Sigma} \cdot \vec{L}^L + 1) - (L + 1)(2L + 1)}{(L + 1)(2L + 1)}, \quad (3.10)$$

$$\Gamma_{L+1}^R = \frac{2(-\vec{\Sigma} \cdot \vec{L}^R + L + 1)(-\vec{\Sigma} \cdot \vec{L}^R + 1) - (L + 1)(2L + 1)}{(L + 1)(2L + 1)}, \quad (3.11)$$

$$\Gamma_{L-1}^L = \frac{2(\vec{\Sigma} \cdot \vec{L}^L - L)(\vec{\Sigma} \cdot \vec{L}^L + 1) - L(2L + 1)}{L(2L + 1)}, \quad (3.12)$$

$$\Gamma_{L-1}^R = \frac{2(\vec{\Sigma} \cdot \vec{L}^R + L)(\vec{\Sigma} \cdot \vec{L}^R - 1) - L(2L + 1)}{L(2L + 1)}, \quad (3.13)$$

$$\Gamma_L^L = \frac{-2(\vec{\Sigma} \cdot \vec{L}^L - L)(\vec{\Sigma} \cdot \vec{L}^L + L + 1) - L(L + 1)}{L(L + 1)}, \quad (3.14)$$

and

$$\Gamma_L^R = \frac{2(\vec{\Sigma} \cdot \vec{L}^R + L)(-\vec{\Sigma} \cdot \vec{L}^R + L + 1) - L(L + 1)}{L(L + 1)}. \quad (3.15)$$

The operators in Eq.(3.10)-Eq.(3.15) are generators of GW algebras and are obtained from left and right projectors to eigenspaces of the total angular momentum, $\vec{L} + \vec{\Sigma}$, where $\vec{\Sigma}$ are the matrices representing the spin 1 representation of $SU(2)$.

The continuum limits of Eq.(3.4)-Eq.(3.6) are

$$D_1 = (\vec{\Sigma} \cdot \vec{\mathcal{L}} - (\vec{\Sigma} \cdot \hat{x})^2 + 2) + 2(\vec{\Sigma} \cdot \hat{x}) + \{\vec{\Sigma} \cdot \vec{\mathcal{L}}, \vec{\Sigma} \cdot \hat{x}\}, \quad (3.16)$$

$$D_2 = (\vec{\Sigma} \cdot \vec{\mathcal{L}} - (\vec{\Sigma} \cdot \hat{x})^2 + 2) - 2(\vec{\Sigma} \cdot \hat{x}) - \{\vec{\Sigma} \cdot \vec{\mathcal{L}}, \vec{\Sigma} \cdot \hat{x}\} \quad (3.17)$$

and

$$D_3 = \vec{\Sigma} \cdot \vec{\mathcal{L}} - (\vec{\Sigma} \cdot \hat{x})^2 + 2. \quad (3.18)$$

The corresponding chirality operators in the continuum are

$$\gamma_1 = (\vec{\Sigma} \cdot \hat{x})^2 + (\vec{\Sigma} \cdot \hat{x}) - 1, \quad (3.19)$$

$$\gamma_2 = (\vec{\Sigma} \cdot \hat{x})^2 - (\vec{\Sigma} \cdot \hat{x}) - 1 \quad (3.20)$$

and

$$\gamma_3 = 1 - 2(\vec{\Sigma} \cdot \hat{x})^2 \quad (3.21)$$

respectively.

Dirac Operator	$L \in \mathbb{Z}$	$L \in \frac{\mathbb{Z}}{2}$
D_1	$4L(2L+1)$	$2L(5L+1)$
D_2	$-4L(2L+1)$	$-2L(5L+1)$
D_3	0	0

Table 1: Traces of the 3 Dirac Operators

The trace of the Dirac operators

The trace of the Dirac operators in Eq.(3.4)-Eq.(3.6) can be computed analytically by using the formula

$$tr(A \otimes B) = tr(A).tr(B) \quad (3.22)$$

where A and B are square matrices. Since the Dirac operators we construct act on $Mat(2L+1) \otimes \mathbb{C}^3$, they are of the form of tensor products and hence we can apply this formula to analytically compute their traces.

The trace is a rotationally invariant object leading to

$$tr((L_1^L)^2) = tr((L_2^L)^2) = tr((L_3^L)^2) \quad (3.23)$$

and

$$tr(\Sigma_1^2) = tr(\Sigma_2^2) = tr(\Sigma_3^2) = 2. \quad (3.24)$$

The above equations hold due to the fact that the three generators of any representation of the $SU(2)$ algebra have the same trace because of rotational invariance.

The trace of $(L_i^L)^2$ varies according to whether L is integer or half-integer. When L is an integer

$$tr((L_i^L)^2) = \frac{1}{3}L(L+1)(2L+1)^2 \quad (3.25)$$

and when L is an half-integer

$$tr((L_i^L)^2) = \frac{1}{3}L(L+1)(L+2)(2L+1). \quad (3.26)$$

The same formulas hold when the left operators in the above equations are replaced by right operators. It is simple to see that $\vec{\Sigma} \cdot \vec{L}^L$ and $\vec{\Sigma} \cdot \vec{L}^R$ are traceless. Using these identities we write down the traces of our 3 Dirac operators in Table(1)

The trace of the Dirac operator is the sum of its eigenvalues. The availability of these exact trace formulas are helpful in verifying the spectrum of these operators found numerically.

The operators D_1 and D_2 have non-zero trace implying the existence of unpaired eigenstates or zero modes.

To check the unitary equivalence of the 3 Dirac operators, it is a necessary, though not sufficient condition that the traces of the 3 operators be the same. Since the trace formulas show the traces are not the same, they provide an analytic proof for the unitary inequivalence of the 3 Dirac operators confirming numerical results.

4. Analytic results of the spectrums of the spin $\frac{1}{2}$ and spin 1 Dirac operators

The spectrum of the spin $\frac{1}{2}$ Dirac operator can be found analytically [3]. In the GW approach to constructing the Dirac operator, the spin $\frac{1}{2}$ system has the same spectrum both in the continuum and the fuzzy level. To illustrate the method of finding the spectrum, we consider the spin $\frac{1}{2}$ Dirac operator in the continuum:

$$D_{\frac{1}{2}} = \vec{\sigma} \cdot \vec{\mathcal{L}} + 1. \quad (4.1)$$

In the above equation $\vec{\mathcal{L}}$ is the orbital angular momentum got by taking the continuum limit of $\vec{L}^L - \vec{L}^R$. $\vec{\sigma}$ are the spin $\frac{1}{2}$ Pauli matrices. The total angular momentum \vec{J} given by

$$\vec{J} = \frac{\vec{\sigma}}{2} + \vec{\mathcal{L}}$$

commutes with the Dirac operator. We can use its eigenvalues to label the eigenstates of the Dirac operator. For given cut-off angular momentum L , the spectrum of the orbital angular momentum is given by

$$\vec{L} \in \{0, 1, \dots, 2L\}. \quad (4.2)$$

Given this we can find the spectrum of the total angular momentum \vec{J} to be

$$\vec{J} \in \left\{ \frac{1}{2}, \frac{3}{2}, \dots, 2L - \frac{1}{2}, 2L + \frac{1}{2} \right\}. \quad (4.3)$$

Each value of the total angular momentum \vec{J} can be got from two different orbital angular momentum except the top mode whose \vec{J} value is $2L + \frac{1}{2}$. From this we can count the total number of eigenvalues for a given cut-off L with the help of the following sum:

$$\sum_{j=\frac{1}{2}}^{j=2L-\frac{1}{2}} 2(2j) + 2L + \frac{1}{2} = 2(2L + 1)^2. \quad (4.4)$$

The spectrum of the Dirac operator in Eq.(4.1) can be got by noting that this operator can be written as

$$D_{\frac{1}{2}} = \vec{J}^2 - \vec{\mathcal{L}}^2 + \frac{1}{4}. \quad (4.5)$$

As $[\vec{J}^2, \vec{\mathcal{L}}^2] = 0$, we can write the spectrum of $D_{\frac{1}{2}}$ as

$$\text{Spectrum of } D_{\frac{1}{2}} = j(j+1) - l(l+1) + \frac{1}{4}. \quad (4.6)$$

As mentioned before each j comes from two different l values except the top mode. Thus we have for the spectrum of $D_{\frac{1}{2}}$:

$$D_{\frac{1}{2}} \left(\begin{array}{l} = j + \frac{1}{2}; \text{ if } l = j - \frac{1}{2} \\ = -j - \frac{1}{2}; \text{ if } l = j + \frac{1}{2}. \end{array} \right) \quad (4.7)$$

The spectrum has the chiral nature as expected. Note that there are no zero modes for the spin $\frac{1}{2}$ Dirac operator. The computation of the spectrum in the spin $\frac{1}{2}$ is easy due to the form of $D_{\frac{1}{2}}$ as given by Eq.(4.1). This however is not true for the Dirac operator of the spin 1 case given by Eq.(3.18). This is due to the presence of the term $\vec{\Sigma} \cdot \hat{x}$ which does not commute with $\vec{\Sigma} \cdot \vec{L}$ making the analytic computation difficult. This is the reason why we take to numerical methods to achieve this. Nevertheless we can still get some vital information about the spectrum of the spin 1 Dirac operator by analytic methods.

The total angular momentum \vec{J} given by

$$\vec{J} = \vec{\Sigma} + \vec{L}$$

commutes with the Dirac operator in Eq.(3.18) just as the corresponding total angular momentum does in the spin $\frac{1}{2}$ case. The spectrum of the orbital angular momentum \vec{L} is the same as in the spin $\frac{1}{2}$ case given by Eq.(4.2). The spectrum of \vec{J} is now given by

$$\vec{J} \in \{0, 1, 2, \dots, 2L-1, 2L, 2L+1\}. \quad (4.8)$$

In this case each value of \vec{J} comes from three different orbital angular momenta namely $j-1$, j and $j+1$ except three j values. $j=0$ comes from only one state. $j=2L$ comes from 2 states and $j=2L+1$ comes from only one state. These are easy to check as they involve the simple angular momentum addition rules. With this information we can count the number of eigenvalues for each cut-off L with the following sum:

$$1 + \sum_{j=1}^{j=2L-1} 3(2j+1) + 2(4L+1) + 2(2L+1) + 1 = 3(2L+1)^2. \quad (4.9)$$

This is exactly the number of eigenvalues we expect from each cut-off L for the spin 1 case as this is the size of the matrix for the Dirac operator for each L . These arguments can be easily extended to the Dirac operators of all spins but we will not do so here.

4.1 Number of positive eigenvalues and Zero modes for the spin 1 Dirac operator

Out of the three Dirac operators in the spin 1 case we will consider the traceless Dirac operator (See Table 1). The trace equation gives us an easy and elegant way to count the number of different non-zero positive and negative eigenvalues as well as the number of zero modes for each cut-off angular momentum L .

The zero modes can be counted as follows: $j=0$ comes from just one orbital angular momentum state and so it can't result in a positive or negative eigenvalue of D_3 and hence it must only be 0 due to the traceless nature of the Dirac operator. This contributes 1 zero mode for each L . Similar argument holds for $j=2L+1$ which contributes $2(2L+1)+1$ zero modes for each L . For values of j between 1 and $2L-1$ there is a contribution of $2j+1$ zero modes for each of the j values. Summing all this we find that there are exactly $(2L+1)^2 + 2$ zero modes for each L .

In a similar way we can find the number of positive eigenvalues. When we do this we find there is a contribution of $2j+1$ eigenvalues for values of j between 1 and $2L$. Summing

these we get $4L^2 + 4L$. As the Dirac operator is traceless, the same argument holds for the negative eigenvalues giving a total of $4L^2 + 4L$ eigenvalues for each L . It is easy to see that the sum of the positive, negative eigenvalues and zero eigenvalues give $3(2L + 1)^2$ as the total number of eigenvalues as expected for each cut-off L .

These arguments can again be easily extended to the spectrum of higher spin Dirac operators on S_F^2 . It is also easy to see that there are no zero modes for half-integral spin systems on S_F^2 as none of the Dirac operators for half-integral spin systems are traceless. We will not discuss them any further in this work except for a few remarks in the end.

Finally we count the number of different positive eigenvalues we expect to find for the spin 1 Dirac operator for each cut-off L . Since there are $2L + 2$ values the total angular momentum j can take, out of which 2 of them can only contribute to the zero modes for each L , we can conclude that there are $2L$ different positive eigenvalues for each L . The degeneracies of each of them can easily be read off as $2j + 1$ according to the corresponding value j takes.

4.2 Remarks on the other two Dirac operators for the spin 1 case

So far the arguments in this section were for the traceless Dirac operator in Eq.(3.18). These arguments do not hold for the Dirac operators in Eq.(3.16) and Eq.(3.17) as they have positive and negative traces respectively. These are given in table 1.

Consider the Dirac operator with the positive trace whose continuum value is given by Eq.(3.16). In this case too we have for the spectrum of the total angular momentum

$$\text{Spec } \vec{J} \in \{0, 1, \dots, 2L - 1, 2L, 2L + 1\} \quad (4.10)$$

as before. However in this case we cannot say that the states corresponding to $j = 2L + 1$ and $j = 0$ correspond to zero modes. This is because of the non-zero trace. They now have some positive energy say E_0 and E_{2L+1} . We then have the following equation

$$E_0 + (4L + 3)E_{2L+1} = 4L(2L + 1) \quad (4.11)$$

for integral values of L and

$$E_0 + (4L + 3)E_{2L+1} = 2L(5L + 1) \quad (4.12)$$

for half-integral values of L . The $4L + 3$ states with energy E_{2L+1} correspond to unpaired eigenstates. If $|E_{2L+1}\rangle$ is the state with energy E_{2L+1} , then these states will be of the form $\gamma^{2k}|E_{2L+1}\rangle$ where γ is the chirality operator given in Eq.(3.19) and k is an integer. In the spin $\frac{1}{2}$ case these states, with the corresponding chirality operator for the spin $\frac{1}{2}$ system, will equal $|E\rangle$ itself as $\gamma^2 = 1$ for the spin $\frac{1}{2}$ case. It can be easily seen from Eq.(3.19) that this is not true for the spin 1 case. So we get the possibility for a number of states with the same energy. With this note, we analyze only the spectrum of the traceless Dirac operator in what follows.

Having studied the general nature of the spectrum for the spin 1 Dirac operator, we compute the eigenvalues numerically in the next section. In particular we will find a relation between the eigenvalue and its multiplicity for a given cut-off L . This is equivalent to finding the eigenvalues as a function of total angular momentum j for each cut-off L .

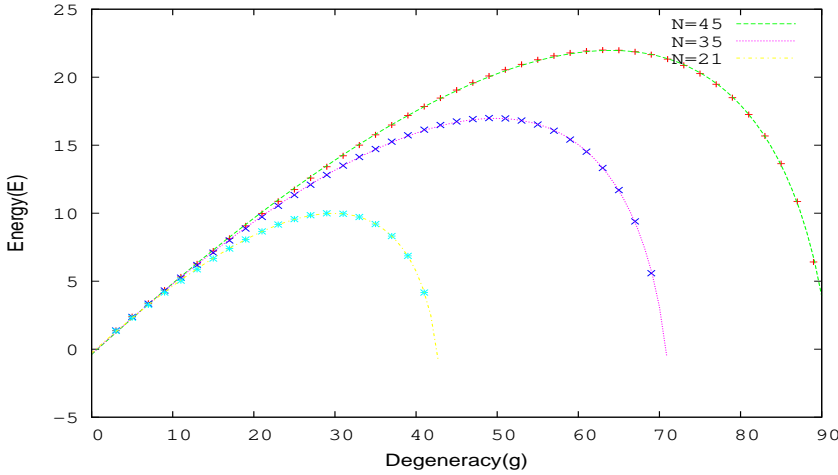


Figure 1: Plot of the energy eigenvalues along with the best fit curves for $N = 21$, $N = 35$ and $N = 45$.

5. Numerical Results

We compute the eigenvalues of the three Dirac operators in Eq.(3.4)-Eq.(3.6) numerically. The size of each of these operators is $3N^2$ where $N = 2L + 1$ and L is the cutoff. It is clear from the dimensions of these matrices ($\sim 9N^4$) that we cannot go to arbitrarily large values of N . Even for $L = 22$, the size of the matrix becomes 6075×6075 which is difficult to handle numerically within the resources available to us. For large values of N number of computational steps increase which will lead to growth of systematic error. However, the patterns emerging from the spectrum we computed so far strongly suggest what the behavior would be at higher values of N . This circumvents computational problems and helps us predict the behavior as we go close to the continuum. This is particularly important given the problems in handling very large matrices.

The nature of the spectrum was discussed in the previous section and we confirm those results numerically. The spectrum of D_3 is similar to that of fermions with equal number of positive and negative energy eigenvalues. This is a reflection of the existence of the chirality operator given by Eq.(3.9), which anticommutes with D_3 . Apart from the non-zero eigenvalues there also exist a number of zero modes. We find exactly $(2L+1)^2 + 2$ zero modes for each cut-off L as we explained in the previous section. The number of positive eigenvalues is also as expected.

We work with only the positive eigenvalues of the spectrum. As the operator is traceless we have the same pattern for the negative eigenvalues and so we do not use them to fit curves. Then we find the degeneracies of each of the positive eigenvalues. Note from the discussion in the earlier section, that there can only be odd degeneracies for our system as the total angular momentum j takes integral values. The plot for the energy vs the degeneracies is shown in figure 1. It shows the data points for three different values of N (namely $N = 21$, $N = 35$ and $N = 45$) along with the best fit curves.

By inspection we found the curve has a mirror symmetry about some principal axis.

Next we try to find a universal curve that will fit the data(eigenvalues) of different cutoffs, just by changing the value of the cutoff. To this end we analyzed the data in a rotated frame in which the data was found to have reflection symmetry around the rotated y-axis. Given that the data for small (E, g) is independent of the cutoff(this can be seen in figure 1 where for small values of g the three sets of data points lie almost on top of each other on a straight line), we found a unique rotation angle to rotate all the results for different cut-off L . After observing the reflection symmetry of (E', g') we tried to fit the data with a polynomial with only even powers. To our surprise we found an excellent fit with just a parabola for all different cutoff values. Higher powers in the function did not make any further improvement in the fitting. The parameters of the parabola run with the cut off. We also find excellent fit for these parameters as a function of the cutoff L .

We now elaborate this method. The plot of (E, g) is rotated to a new set of variables (E', g') . This set of points is then fitted with the curve

$$E' = \alpha(g' + \eta)^2 + \beta. \quad (5.1)$$

Here α , β and η are expected to vary with the cut-off L . The relation between (E', g') and (E, g) is given by

$$\begin{pmatrix} E' \\ g' \end{pmatrix} = \begin{pmatrix} \cos \theta & \sin \theta \\ -\sin \theta & \cos \theta \end{pmatrix} \begin{pmatrix} E \\ g \end{pmatrix}. \quad (5.2)$$

The angle $\theta = 2.26159$ radians. This angle is a constant for different values of L . This can be seen as a consequence of the data points lying on top of each other for small values of g as seen in figure 1. Note that E' and g' are not energies and degeneracies respectively. We just need to use the transformation in Eq.(5.2) to get the relation between the energies and the degeneracies.

Our next task is to find α , β and η as functions of $N = 2L + 1$. They are found by fitting the quadratic form (Eq.(5.1)) to the rotated curves for different values of N . We find them to follow simple relations. These are shown in the figures 2. The exact functions we found were:

$$\alpha = \frac{0.863569}{N^{0.930775}} - 0.00141635, \quad (5.3)$$

$$\beta = -1.45123N + 0.333497 \quad (5.4)$$

and

$$\eta = -1.16288N - 0.555529. \quad (5.5)$$

The numbers may look uninteresting but if we could fit these functions after we find these parameters for more values of N we could converge onto some special numbers. We did not attempt this in this work. The relations are simple enough to imply something deeper in the spectrum. More exact numbers could help in the quest for an analytic solution of this problem.

We can now write down the exact relation between E and g based on our numerical fits:

$$E = \frac{\sqrt{b(g)^2 - 4ac(g)} - b(g)}{2a} \quad (5.6)$$

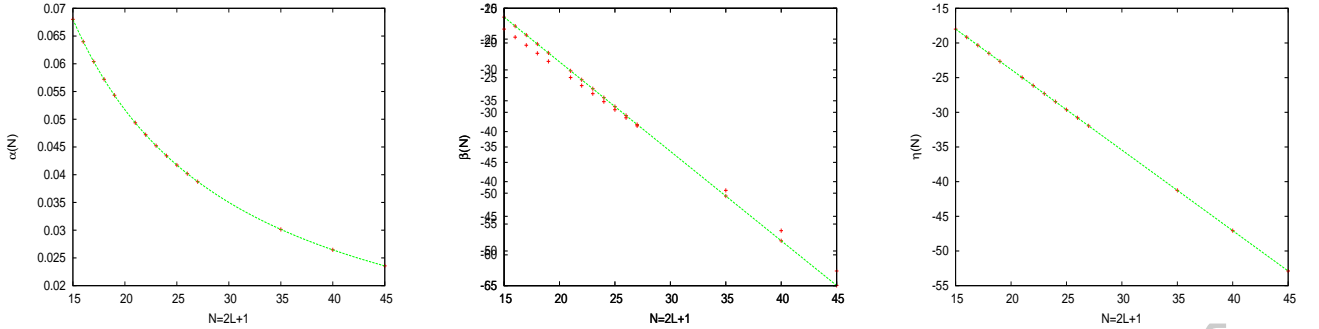


Figure 2: Parameters α , β and η as a function of N .

where

$$a = \alpha \cos^2 \theta, \quad (5.7)$$

$$b(g) = 2\alpha \cos \theta (\sin \theta g + \eta) + \sin \theta \quad (5.8)$$

and

$$c(g) = \alpha (\sin \theta g + \eta)^2 + \beta - \cos \theta g. \quad (5.9)$$

Having found this relation between E and g , we can now find the eigenvalues for arbitrarily large values of N . If we diagonalize D_3 for such large values of N it would take a lot of memory on the computer and is subject to a lot of numerical error. But we can get around this with our relation between E and g . Figure 3 shows the eigenvalues for $N = 60$. Note that though the curve looks continuous, we have seen in the previous section that degeneracies are allowed to take only odd integral values. The maximum degeneracy for a given N is $2N - 1$. Starting from 3 we can allow g to vary till $2N - 1$ through odd integers and find the corresponding eigenvalues using Eq.(5.6). In an equivalent manner we can find the energy eigenvalues as a function of the total angular momentum j by simply substituting $g = 2j + 1$ in Eq.(5.6).

6. Conclusions

The spectrums of the spin 1 Dirac operators are found numerically. The three operators do not have the same spectrum making them unitarily inequivalent. This may have interesting consequences which we plan to explore in the future. The fermionic character of the spectrum is noteworthy as there exists no such higher dimensional analog in the Minkowski case. We expect this behavior also for higher spin Dirac operators on S_F^2 as they all come paired with an anticommuting chirality operator.

The universal relation between the energy eigenvalues and their degeneracies we find in Eq.(5.6) is indeed remarkable as it circumvents what would have been an almost impossible computational problem involving large matrices. This now allows us to find the eigenvalues for any arbitrarily large cut-off L . The simple relation between the eigenvalues

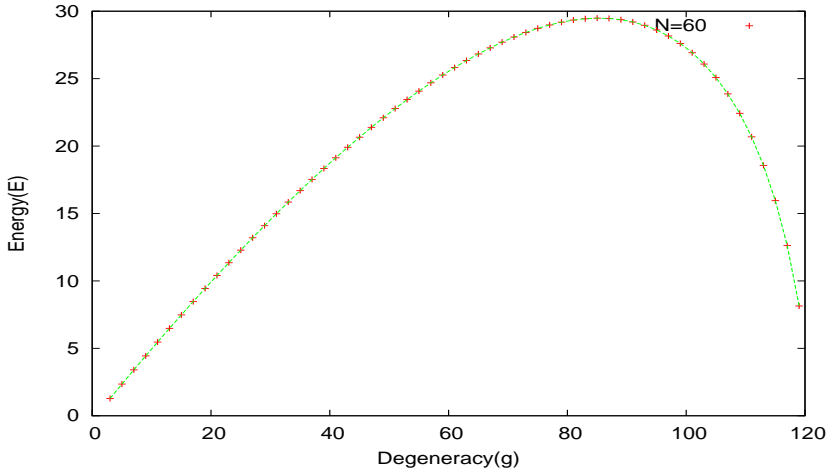


Figure 3: Plot predicting the energy eigenvalues for $N = 60$.

and their degeneracies seem to suggest some connection with the underlying symmetry in the problem.

Having obtained the spectrum for the spin 1 Dirac operator for arbitrarily large cut-off L , we can go on to find the partition function for a system of particles occupying these energy levels. Assuming fermionic statistics we can compute several thermodynamic quantities for this system. Several interesting features arise and these are reported in [15].

A quantum particle on the continuum sphere, S^2 has energy eigenvalues given by $l(l + 1)$. These are the eigenvalues of the Laplacian on the sphere which is a second order differential operator. The eigenvalues of the square of the continuum limit of the spin $\frac{1}{2}$ Dirac operator on S_F^2 [16, 1, 3, 17] also gives a spectrum similar to that of the standard Laplacian on S^2 apart from a additional constant. This additional constant can be interpreted as the scalar curvature according to the Lichnerowicz formula for the square of a general Dirac operator. In the Minkowskian case this is analogous to the square of the Dirac operator giving the Laplacian on that space. This leads to each component of the Dirac spinor satisfying the Klein-Gordon equation. We can view the Laplacian of the standard sphere as an analog of the Klein-Gordon equation on the sphere as this gives the $SU(2)$ covariant dispersion relation on S^2 . Note that we can add additional constants to this Laplacian as they are rotationally invariant. This however is not true for any of the 3 spin 1 Dirac operators on S_F^2 as their continuum limits, given by Eq.(3.16)-Eq.(3.18), contain $\vec{\Sigma} \cdot \hat{x}$ terms which makes the square of these operators look complicated. (Note that we do still get $l(l + 1)$, but with additional terms containing $\vec{\Sigma} \cdot \hat{x}$ which makes the analytical computation of the spectrum difficult.) Thus the spectrum of their squares are not the standard one making the study of these deviations interesting as there exist no counterparts on higher dimensional Minkowskian space.

We are also computing the spectral action of these Dirac operators. This will be compared with the spectral action of the spin $\frac{1}{2}$ Dirac operator on the continuum sphere. This kind of analysis was carried out recently [14] where interesting connections were made

with cosmology. The results will be reported in a future work [18].

It was found in [1], that for a given chirality operator there exist several different Dirac operators. However this was done in the continuum limit and we have not found their fuzzy analogs. These will most certainly not be unitarily equivalent. This seems to be a new property of spin systems on S_F^2 and they need to be studied further.

7. Acknowledgements

We thank Prof.A.P.Balachandran, Prof.T.R.Govindarajan and Prof. Satyavani Vemparala for useful discussions and references. We also thank Prof.Xavier Martin for useful comments. PP thanks Prof.T.R.Govindarajan for the hospitality at IMSc, Chennai. This work was supported in part by DOE under the grant number DE-FG02-85ER40231.

References

- [1] A.P.Balachandran, P. Padmanabhan, *Spin j Dirac Operators on the Fuzzy 2-Sphere*, JHEP 0909:120,2009 and arXiv:0907.2977v2 [hep-th].
- [2] John Madore, *The fuzzy sphere*, 1992 Class. Quantum Grav. 9 69.
- [3] A.P. Balachandran, S. Kurkcuoglu, S. Vaidya, *Lectures on fuzzy and fuzzy SUSY physics*, World Scientific Publishing(2007).
- [4] M. Panero, *Numerical simulations of a non-commutative theory: The scalar model on the fuzzy sphere*, JHEP **0705** (2007) 082.
- [5] M. Panero, *Quantum Field Theory in a Non-Commutative Space: Theoretical Predictions and Numerical Results on the Fuzzy Sphere*, SIGMA 2:081,2006 and arXiv:hep-th/0609205v2.
- [6] C.R. Das, S. Digal, and T.R. Govindarajan, *Finite temperature phase transition of a single scalar field on a fuzzy sphere*, Mod. Phys. Lett. **A** **23** (2008) 1781.
- [7] C.R. Das, S. Digal, and T.R. Govindarajan, *Spontaneous symmetry breakdown in fuzzy spheres*, arXiv:0801.4479v2.
- [8] F. G. Flores, X. Martin, and D. O'Connor, *Simulation of a scalar field on a fuzzy sphere*, arXiv:0903.1986v1.
- [9] D. O'Connor and B. Ydri, *Monte Carlo simulation of a nc gauge theory on the fuzzy sphere*, JHEP **0611** (2006) 016.
- [10] T.Kawano, K.Okuyama, *Matrix theory on noncommutative torus*, Physics Letters B, Volume 433, Number 1, 6 August 1998 , pp. 29-34(6).
- [11] M.Chaichian, A.Demichev, P.Presnajder, *Field Theory on Noncommutative Space-Time and the Deformed Virasoro Algebra*, arXiv:hep-th/0003270v2.
- [12] T.R.Govindarajan, P. Padmanabhan, T.Shreecharan, *Beyond Fuzzy Spheres*, To appear in J.Phys. A and arXiv:0906.1660v2 [hep-th].
- [13] A. Connes, *Noncommutative Geometry*, Academic Press, London, 1994.
- [14] Jingbo Wang, Yanshen Wang, *Spectral action on a fuzzy sphere*, 2009 Class. Quantum Grav. 26 155008.

- [15] S. Digal, P. Padmanabhan, *Unusual Thermodynamics on the Fuzzy 2-Sphere*, arXiv:1006.4792v1 [hep-th].
- [16] U. Carow-Watamura and S. Watamura, *Chirality and Dirac Operator on Noncommutative Sphere*, Commun. Math. Phys. 183 (1997) 365 and hep-th/9605003; *Noncommutative Geometry and Gauge Theory on Fuzzy Sphere*, Commun. Math. Phys. 212 (2000) 395 and hep-th/9801195.
- [17] H. Grosse, C. Klimck, P. Prenajder, *Topologically nontrivial field configurations in noncommutative geometry*, Commun. Math. Phys. 507 (1996) and hep-th/9510083.
- [18] S. Digal, P. Padmanabhan, *In Preparation*.